

Encapsulation of ibuprofen over mesoporous nanocrystalline hollow silica cuboids

N Venkatathri*, M Nookaraju, A Rajini & I A K Reddy

Department of Chemistry, National Institute of Technology
Warangal, Warangal 506 004, Andhra Pradesh, India
Email: venkatathrin@yahoo.com

Received 29 March 2012; revised and accepted 17 April 2013

Nanocrystalline hollow nano silica cuboids and MCM-41 have been synthesized and characterized using small angle powder X-ray diffraction, scanning electron micrograph, transmission electron micrograph, thermogravimetry/differential thermal analysis, Fourier transform infrared spectroscopy, nitrogen adsorption-desorption and ibuprofen adsorption followed ultraviolet spectroscopic analysis. The results indicate that mesoporous silica nanohollow cuboids store much more guest molecules than conventional nanocrystalline mesoporous Si-MCM-41.

Keywords: Silica, Mesoporous nano hollow cuboids, Cuboids, Hollow cuboids, Ibuprofen, Mesoporous materials

Since the discovery of mesoporous silica molecular sieves by Beck *et al.*^{1,2} mesoporous materials have opened many new possibilities for application in the fields of catalysis³, separation and nanoscience⁴⁻⁷. In recent years, fabrication of silica materials with designed structure (e.g. thin films, monoliths, hexagonal prisms, toroids, discoids, spirals, dodecahedron and hollow sphere shapes) has been an important area of research in modern materials chemistry. Amongst these, the fabrication of monodispersed hollow spheres with control size and shape is a fastest developing area⁸⁻¹⁰. It is generally accepted that hollow spheres with mesopores will exhibit more advantages in mass diffusion and transportation as compared with conventional hollow spheres with solid shell. They can serve as a small container for application in catalysis and control release studies^{11,12}. The methods currently used to fabricate a wide range of stable hollow spheres include nozzle reactor processes, emulsion/phase separation, sol-gel processing and sacrificial core techniques. The fabrication of hollow spheres has been greatly impacted by the layer-by-layer (LbL) self-assembly technique¹³. This method allows the construction of composite multilayer assemblies based on the electrostatic attraction between

nanoparticles and oppositely charged polyions. By varying the synthetic methodology and reactants, it is possible to achieve materials with interesting morphology and properties.

The presence of pores of uniform size lined with silanol groups make these mesoporous materials a potential candidate for hosting a variety of guest chemical species such as organic molecules, semiconductor clusters and polymers¹⁴. For example, MCM-41 was reported as a drug delivery system¹⁵. Ibuprofen has been shown to be readily adsorbed from an *n*-hexane solution into the porous matrix of MCM-41, and slowly released into a solution simulating physiological fluid (SPF). Furthermore, it has been found that in this host/guest system there is a strong interaction between the silanol groups and the carboxylic acid of the ibuprofen molecule. In view of the feasibility of this system for drug retention and delivery, further efforts are required to control the amount of drug delivered and its release rate. It is possible that the delivery rate can be modulated by modifying the interaction between the confined molecule and the mesoporous matrix with different morphology. Here, one of the advantages of nanocuboids compared to conventional mesoporous materials is reflected in their much higher storage capacity. In the present study, ibuprofen with the molecules size of 1.0×0.6 nm was used to examine the storage capacity.

Mesoporous hollow silica spheres are important due to their drug storage property. Synthesis of mesoporous silica nano hollow cuboids is a very recent advancement¹⁶. In the present study, the physicochemical properties of mesoporous silica nanocrystalline MCM-41 and nanohollow cuboids are compared and the ibuprofen drug storage property of both the materials is studied.

Experimental

Silica nanohollow cuboids were synthesized as follows. Triethanolamine (3.57 mL, TEA, 98%, Aldrich, USA) was added to a solution containing 74 mL of ethanol (99%, Aldrich, USA) and 10 mL of deionized water. Tetraethoxyorthosilicates (6 mL, TEOS, 98%, Aldrich, USA) was added to the above mixture at 298 K with vigorous stirring. The reaction mixture was stirred for another 1 h.

A solution containing 5 mL of TEOS and 2 mL of octadecyltrimethoxy silane (C18TMS, 90%, Aldrich, USA) was added to the above solution (11.4 SiO₂: 6 TEtA: 1 C18TMS: 149 H₂O: 297.5 EtOH) and further reacted for 24 h. The resulting octadecyl group incorporated silica nanocomposite was retrieved by centrifugation. The sample was washed several times with distilled water, dried and calcined at 823 K for 8 h in air to obtain hollow cuboids silica material.

Nanocrystalline silica MCM-41 was synthesized as reported by Grun *et al.*¹⁷ Cetyltrimethylammonium bromide was dissolved in 120 g of deionized water to yield a 0.055 mol L⁻¹ solution, and to this was added 9.5 g of aqueous ammonia (25 wt%, 0.14 mol). While stirring, 10 g of tetraethoxy silane (0.05 mol) was added slowly to the surfactant solution over a period of 15 min, resulting in a gel with the following molar composition: TEOS (1):cetyltrimethylammonium bromide (0.152):NH₃ (2.8):H₂O (141.2). The mixture was stirred for one hour and the white precipitate was filtered and washed with 100 mL of deionized water. After drying at 373 K for 12 h, the sample was heated to 823 K (rate: 1 K min⁻¹) in air and kept at this temperature for 5 h to remove the entrapped template.

X-ray diffractograms (XRD) were recorded on Rigaku Multiplex diffractometer using Cu-K radiation and a proportional counter as detector. A divergence slit of 1/328 on the primary optics and an anti-scatter slit of 1/168 on the secondary optics were employed to measure data in the low angle region. The particle size and shape were analyzed by a scanning electron microscope (SEM) Topcon SM-300. Transmission electron micrographs (TEM) of the samples were scanned on a JEOL JSM-2000 EX electron microscope operated at 200 kV. The samples for TEM were dispersed in isopropyl alcohol, deposited on a Cu-grid and dried. Thermogravimetry (TG) analysis of the crystalline phase was performed on an automatic derivatograph (Setaram TG 92). The specific surface area (BET) of the samples was determined using a Micromeritics ASAP 2010 volumetric adsorption analyzer. Before N₂ adsorption, the samples were evacuated in vacuum at 523 K for 5 h. The data points of p/p_0 in the range of 0.05–0.3 were used for calculation of specific surface area. The Fourier transform infrared (FT-IR) spectra in the framework region were recorded in the diffuse reflectance mode (Nicolet 60SXB) using 1:300 ratio of sample with KBr pellets. Ultraviolet-visible (UV-vis) spectroscopic analyses were carried out on a Shimadzu UV-2450 spectrometer.

Ibuprofen (IBU) drug (Ranbaxy Chem. Ltd., 99%) was dissolved in hexane at a concentration of 30 mg/mL. The nanocuboids or MCM-41 (1.0 g) was added to 50 mL IBU hexane solution at room temperature. The vials were sealed to prevent the evaporation of hexane and then the mixture was stirred for 24 h. The nanocuboids or MCM-41 adsorbed with IBU were separated from this solution by centrifugation and dried under vacuum at 60 °C. The filtrate (1.0 mL) was extracted from the vial, diluted to 10 mL and then analyzed by UV-vis spectroscopy at a wavelength of 235–320 nm.

Results and discussion

Tetraethylorthosilicate (TEOS) was hydrolyzed in the presence of basic triethanolamine. However, the hydrolysis rate of TEOS using triethanolamine is very slow as compared to hydrolysis with NH₃. For example, using the molar ratio described above, TEOS could be hydrolyzed in 2 h using NH₃ whereas triethanolamine took 24 h to hydrolyze the TEOS. In the present synthetic recipe, triethanolamine acts not only as a catalyst for the hydrolysis but also as a reactant. The hydrolyzed silica monomers react with triethanolamine to give the respective oxide. Such silicate-triethanolamine adducts are held together by hydrogen bonding. The triethanolamine sandwiched silica layer condenses and form nanocuboids. MCM-41 is reported to crystallize by self-assembly of surfactant/template¹⁷, similar to nanocuboids.

The X-ray diffraction patterns of the calcined MCM-41 and hollow cuboids are given in Fig. 1 (a, b). The pattern from as-synthesized sample did not change much on calcination. The XRD patterns of both as-synthesized and calcined hollow cuboid show three Bragg diffraction peaks, which can be assigned to the (100), (110) and (200) reflections of a hexagonal symmetry structure (*P6mm*) typical for MCM-41. The *d* spacing and unit cell parameter (*a*₀) calculated from the XRD data are 12.6 nm and 14.54 nm respectively¹⁸.

Scanning electron micrographs of MCM-41 and hollow cuboids (Fig. 2) show the particle size of MCM-41 to be 200–500 nm with spherical shape, while the hollow cuboids are aggregates of cuboids with particle size as 500 nm.

Transmission electron micrographs of MCM-41 and hollow cuboids are given in Fig. 3 (a, b). MCM-41 shows hexagonal array of channels, characteristic of mesoporous structure. By Fast

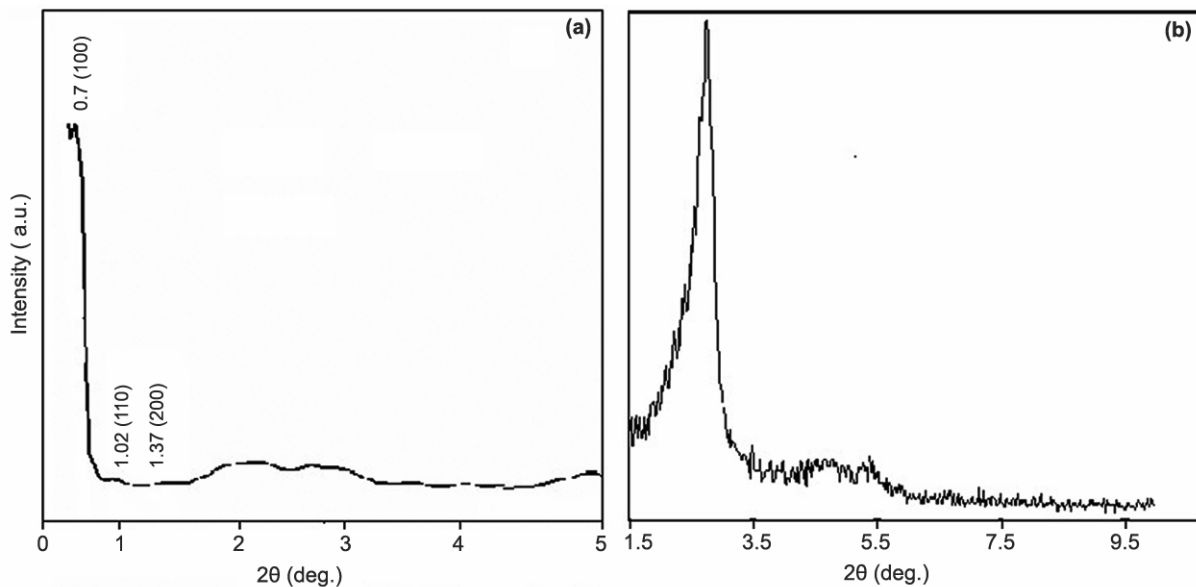


Fig. 1—X-ray diffraction patterns of calcined mesoporous silica. [(a) nanohollow cuboids; (b) nanocrystalline MCM-41].

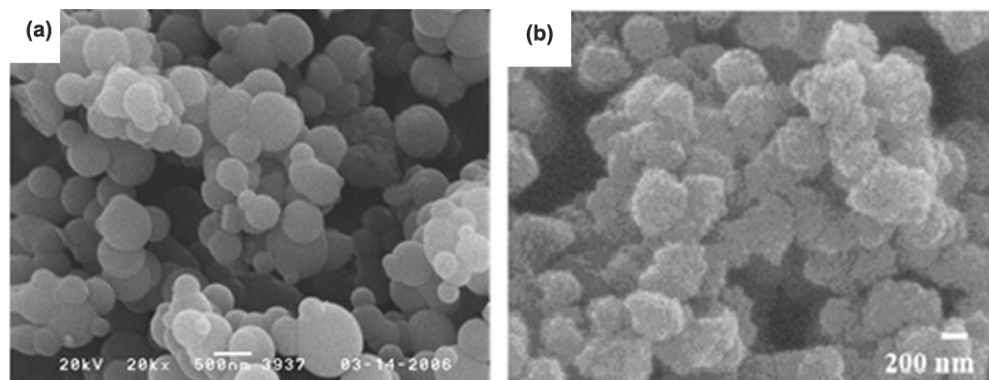


Fig. 2—Scanning electron micrographs of calcined mesoporous silica. [(a) nanocrystalline MCM-41; (b) nanohollow cuboids].

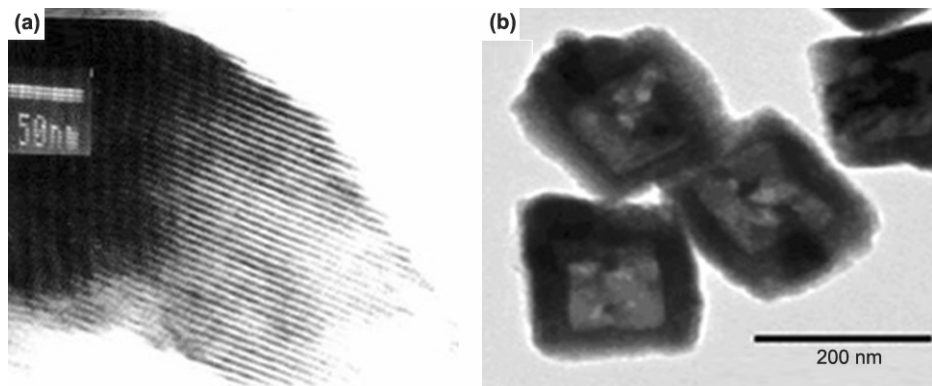


Fig. 3—Transmission electron micrographs of calcined mesoporous silica. [(a) nanocrystalline MCM-41; (b) nanohollow cuboids].

Fourier Transform (FFT) of the TEM images, we estimated the pore size as 3.3 nm. Core and shell structure of the cuboids has been observed from the TEM. It can be seen from the images that the average inner diameter of the cuboids are nearly 100 nm, with outer shell thickness of 50 nm. The particle sizes are uniform as also shown by SEM images. This pore channel arrangement with most running through the shell, are favorable for the access of guest molecules.

Thermograms of MCM-41 and hollow cuboids show 30% loss at 25–625 °C in the case of MCM-41, indicating removal of the template. The initial endothermic loss is due to loss of physisorbed water. Later the exothermic loss is due to oxidative decomposition of template. The TG curve shows that the cuboids begin to lose weight at the beginning of heating because of desorption of the physisorbed water and ethanol. It eliminates almost 25% of its weight in the temperature range 25–200 °C and loses almost 30% weight in the temperature range of 200–500 °C. The second weight loss is due to the oxidative decomposition of the template.

Typical nitrogen sorption isotherms for MCM-41 and hollow cuboids are shown in Supplementary data, Fig S1. In the case of MCM-41, the nitrogen adsorption-desorption isotherms indicate a linear increase of the amount of adsorbed nitrogen at low pressures ($p/p_0 = 0.35$). The resulting isotherm resembles a typical type IV isotherm with a type H2 hysteresis, according to the IUPAC nomenclature^{19–22}. The steep increase in nitrogen uptake at relative pressures in the range between $p/p_0 = 0.40$ and 0.60 is reflected in a narrow pore size distribution. Thus, the difference between nanocrystalline MCM-41 and hollow silica in the solution during the growth process enables one to adjust and to control pore structural parameters such as the specific surface area ($900 \text{ m}^2 \text{ g}^{-1}$), the specific pore volume ($1.29 \text{ cm}^3 \text{ g}^{-1}$), the average pore diameter (239 Å) and medium pore width (302 Å). The nitrogen adsorption-desorption isotherms of nanocuboid is of type IV nature and exhibits a H1 hysteresis loop, which is typical of mesoporous solid²³. Furthermore, the adsorption branch of the isotherm shows a sharp inflection at a relative pressure value of ~0.68. This is characteristic of capillary condensation within uniform pores. The position of the inflection point indicates mesoporous structure, while the sharpness of these

steps indicates the uniformity of the mesoporous size distribution. Correspondingly, the pore size distribution of the calcined sample shows a narrow pore distribution with a mean value of 1.90 nm. The sample with a specific surface area of $792 \text{ m}^2 \text{ g}^{-1}$ and pore volume of $0.51 \text{ cm}^3 \text{ g}^{-1}$ was obtained using the Brunauer-Emmett-Teller (BET) and Barrett-Joyner-Halenda (BJH) methods, respectively.

The Fourier transform infrared spectra of as-synthesized MCM-41 and hollow cuboids show peaks around 1700 and 3430 cm^{-1} , corresponding to the carboxyl and hydroxyl group respectively²⁴. The absorption peak belonging to the Si-O stretching vibration of Si-OH bond²⁵ appears at 960 cm^{-1} . The weak peaks at 2855 and 2920 cm^{-1} belong to the stretching vibrations of C-H bonds, which show that few organic groups are adsorbed on the spheres. The peaks for carboxyl, hydroxyl and C-H vibrations are weak in MCM-41, show lesser organic part resulting from the organic template. The strong peaks near 1100, 802 and 467 cm^{-1} agree to the Si-O-Si bond, which implies the condensation of silicon source²⁶.

Figure 4 shows the UV absorbance spectra of 30 mg/mL ibuprofen hexane solutions²⁷ before and after the interaction with nanocuboid and MCM-41.

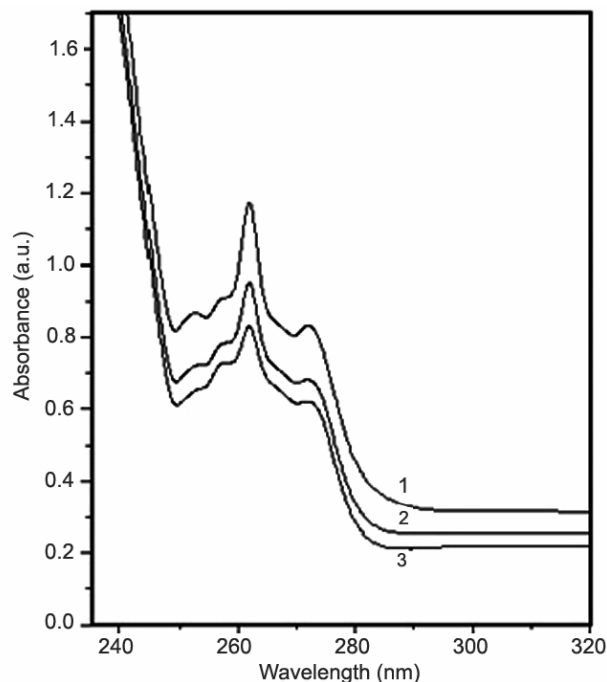


Fig. 4—Ultraviolet-visible absorbance spectra of 30 mg/mL ibuprofen hexane solutions [before (1) and after (2) interaction with calcined mesoporous silica nanohollow cuboids, and (3) mesoporous silica nanocrystalline MCM-41].

The absorbance maximum of ibuprofen remains unchanged after the interaction of the drug with nanocuboid and MCM-41 and no new bands appear indicating no degradation of the drug. The ultraviolet absorbance intensity of the filtrate decreases after interaction of ibuprofen solution with nanocuboids and MCM-41. This shows that the remaining ibuprofen is adsorbed over the molecular sieves. It was calculated that 561.8 mg and 270.5 mg ibuprofen molecules can be stored in per gram nanocuboid and MCM-41, respectively from ultraviolet absorbance according to Beer-Lambert law²⁸. The surface area and pore volume of MCM-41 are close to that of the nanocuboid, but much more ibuprofen molecules can be stored into the nanocuboids than into MCM-41.

In the present study, mesoporous nanocrystalline hollow nano silica cuboids and Si-MCM-41 were synthesized by reported procedures and characterized in detail. Ibuprofen encapsulation studies shows hollow nano silica cuboids store much more ibuprofen molecules compared to Si-MCM-41.

Supplementary data

Supplementary data associated with this article, i.e., Fig. S1, is available in the electronic form at [http://www.niscair.res.in/jinfo/ijca/IJCA_52A\(05\)619-623_SupplData.pdf](http://www.niscair.res.in/jinfo/ijca/IJCA_52A(05)619-623_SupplData.pdf).

References

- 1 Beck J S, Vartuli J C, Roth W J, Leonawicz M E & Kresge C T, *J Am Chem Soc*, 114 (1992) 10834.
- 2 Kresge C T, Leonawicz M E, Roth W J, Vartuli J C & Beck J S, *Nature*, 359 (1992) 710.
- 3 Tanev P T, Chibwe M & Pinnavaia T P, *Nature*, 368 (1994) 321.
- 4 Wu C G & Bein T, *Chem Mater*, 6 (1994) 1109.
- 5 Agger J R, Anderson M W & Pemble M E, *J Phys Chem B*, 102 (1998) 3345.
- 6 Li Y, Shi J, Hua Z, Chen H, Ruan M & Yan D, *Nano Lett*, 3 (2003) 609.
- 7 Yu K, Guo Y, Ding X, Zhao J, Wang Z, *Mater Lett*, 59 (2005) 4013.
- 8 Schacht S, Huo Q, Voigt-Martin I G, Stucky G D & Schuth F, *Science*, 273 (1996) 768.
- 9 Bruinsma P J, Kim A Y & Liu J, *Chem Mater*, 9 (1997) 2507.
- 10 Fowler C E, Khushalani D & Mann S, *Chem Comm*, (2001) 2028.
- 11 Mathlowitz E, Jacob J S, Jong Y S, Carino G P, Chickering D E, Chaturvedi P, Santos C A, Vijayaraghavan K, Montgomery S, Bassett M & Morrell C, *Nature*, 386 (1997) 410.
- 12 Huang H & Remsen E E, *J Am Chem Soc*, 121 (1999) 3805.
- 13 Decher G, *Science*, 277 (1997) 1232.
- 14 Moller K & Bein T, *Chem Mater*, 10 (1998) 2950.
- 15 Vallet-Regi M, Ramila A, del Real R P & Perez-Pariente J, *Chem Mater*, 13 (2001) 308.
- 16 Venkatathri N, Srivastava R, Yun D S & Yoo J W, *Micropor Mesopor Mat*, 112 (2008) 147.
- 17 Grun M, Unger K K, Matsumoto A & Tsutsumi K, *Micropor Mesopor Mat*, 27 (1999) 207.
- 18 Zhao D, Feng J, Huo Q, Melosh N, Fredrickson G H, Chmelka B F & Stucky G D, *Science*, 279 (1998) 548.
- 19 Fujiwara M, Shiokawa K, Tanaka Y & Nakahara Y, *Chem Mater*, 16 (2004) 5420.
- 20 Brunauer S, Deming L S, Deming W S & Teller E, *J Am Chem Soc*, 62 (1940) 1723.
- 21 De Boer J H, *The Structure and Properties of Porous Materials*, (Butterworths, London) 1958.
- 22 IUPAC, *Reporting Physisorption Data for Gas/Solid Systems*, *Pure Appl Chem*, 87 (1957) 603.
- 23 Wu P, Tatsumi T, Komatsu T & Yashima T, *Chem Mater*, 14 (2002) 1657.
- 24 Li Y, Xu C, Wei B, Zhang X, Zheng M, Wu D & Ajayan P M, *Chem Mater*, 14 (2002) 483.
- 25 Shan Y, Gao L & Zheng S, *Mater Chem Phys*, 88 (2004) 192.
- 26 Agger J R, Anderson M W, Pemble M E, Terasaki O & Nozue Y, *J Phys Chem B*, 102 (1998) 3345.
- 27 Zhu Y, Shi J, Chen H, Shen W & Dong X, *Micropor Mesopor Mat*, 84 (2005) 218.
- 28 Jeffery G H, Bassett J, Mendham J & Denney R C, *Vogel's Textbook of Quantitative Chemical Analysis*, (Wesley Longman Limited, UK) 1997, p. 649.